Journal of Advanced Research in Applied Sciences and Engineering Technology

Journal homepage: https://jaraset.com/
ISSN: 2462-1943

MHD RADIATIVE NANOFLUID FLOW IN A VERTICAL PERMEABLE CHANNEL FILLED WITH POROUS MEDIUM

SHYAM MANOHAR [1*], **Dr. SHWETA BOHRA** [2]

[1] *Research scholar, Department of Mathematics, Sangam University, Rajasthan, India*
[2] *Associate Professor, Department of Mathematics, Sangam University, Rajasthan, India*

ARTICLE INFO

Article history:
Received: 12-06-2024
Received in revised form: 12-08-2024
Accepted: 15-09-2024
Available online: 10-01-2025

Keywords:
MHD, thermal radiation, nanofluid, Crank-Nicolson implicit diference.

ABSTRACT

The study of free convective MHD Couette flow of nanofluid between a vertical permeable channel is investigated in the prsence of thermal radiation effect and suction/injection through porous medium. Cu-ethyleneglycol is considered for analysis. Crank-Nicolson implicit diference method is used to solve system of governing unsteady, coupled equations. Also the flow and heat transfer for steady state of this mathematical model is also investigated. A comparetive study for both the cases steady and unsteady is analyzed and disscussed. For both the cases, effect of various physical parameters on velocity distribution, temperature distrtibuiton is depicted graphically.

Introduction

The transient behaviour of a natural convection flow between vertical or horizontal channel has its applications in technological processes. Channel flows are important and occurs in many industrial and engineering applications. Transient free convection MHD flows with radiation have attracted the interest of many researchers in view of their applications in modern materials processing. Moreover, many reseachers have studied flow and heat transfer through vertical parallel porous plates, vertical channel.Study of natural convective flow in two regions one is fiiled with micropolar fluis and one is from viscous fluid in vertical channel has been investigated by Kumar et al. [1]. Further, the effect of inertial force in mixed convection flow between vertical channel in porous medium was numerically investigated by Umavathi et al. [2] taking into account the effect of Darcy an viscous dissipations.Hussanam et al.[3] and Khalid et al. [4] have studied unsteady MHD conjugate flow for different fluids over an oscillating vertical

plate embedded in a porous medium. MHD Couette motion of an electrically conducting, viscous incompressible fluid through saturated porous medium bounded by two insulated vertical porous plates is analyzed by Khem et al. [5]. Jha et al. [6-7] obtainedthe sloution for the problem of transient natural convective Couette flow between two infinite vertical parallel plates. Kataria and Patel [8, 9] has anayzed the effect of radiation, chemical raction, Soret and heat generation effect on MHD free convective Casson fluid flow past an oscillating vertical.

The unsteady MHD free-convection flow governed by the impact of suction or injection is one of the distinguished present-day themes. In many engineering processes suction/injection is used to cool the surface remove/add the reactants and prevent corrosion, thermal oil recoverys, design of thrust bearing. Attia [10] examined the Couette flow and heat transfer with the effect of suction and injection by taking in account of variable properties. Rundora and Makinde [11] studiedthe effct of suction/injection on unsteady fluid flow between two parallel plates in a porous medium with convective boundary condtions. They have taken third grade fluid and variable viscosity. Jha et al. [12, 13] has given both anayltical and numerical solution for Couette flow of viscous incompressible fluid between two infinite vertical porous plates and vertical channel respectively.

For the above studies nanofluid is not considered but for the enhancement in heat transfer, the idea of improving heat transfer performance of fluids with the inclusion of solid particles was first introduced by Maxwell [14]. Suspensions involving mille or micro sized particles create problems, such as fast sedimentation, clogging of channels, high pressure drop, and severe erosion of system boundaries. To overcome these problems, Choi and Eastman [15] used ultrafine nanoparticles with base fluid known as nanofluid.Buddakkagariand Kumar [16] studied two-dimensional transient hydrodynamic boundary layer flow of nanofluid past a cone and plate with constant boundary conditions by using Crank Nicolson implicit diference method. By appliying this same method Chouhan and Kumar[17] obserevd the radiation effect on unsteady flow with velocity and temperature slip boundary conditions in a porous medium channel.Intensive attention has been directed at numerical simulations of convectiveboundary layer flow and heat transfer in nanofluids through vertical plate orchannels with or without MHD, radiation and other effectsby several researchers such as [18-29].Many researchers as [30-33] have been studied mixed convective magneto hydrodynamic water based nanofluid the

different geometries like vertical channel, stretching sheet, inclined duct, cylinder, inclined cylinder & wavy channel etc.

The present work is aimed to investigatefree convective MHD Couette flow of nanofluid between a vertical permeable channel in the prsence of thermal radiation effect and suction/injection through porous medium. The investigation is done for both steady and unsteady flow and heat tranfer under same boundary conditions. The results obtained are found well in agreement with prsent literature.

Mathematical Formulation

In this present study, we consider unsteady free convective Couette flow of a between a vertical channel formed by two infinite porous plates embedded by porous medium in the presence of tranverse magnetic field $B_0$and radiation flux of intensity q_r. We assume that the induced magnetic field is not considered, as the magnetic Reynolds number is taken very small.. The Ohmic heating, ionslip and Hall effects are neglected as they are also assumed to be small. Ethylene glycol based containing Copper nanoparticles is taken for investigation. The nanoparticles spherical shape and size are assumed to be uniform and are in thermal equilibriumwith base fluid.

We take the Cartesian coordinate system (x', y') in such a way that x'-axis is along the moving vertical plate in upward direction, y'-axis is normal to the plane of the plate. Since the porous plates are infinite in extent, the velocity and time are functions of y' and t' only. The fluid and the porous plates of the channel are initially at rest and the whole system is kept at a constant temperature T_0. A porous plate which is situated at $y' = 0$ starts moving along x' direction with a velocity U at $t' \geq 0$ and at the same time temperature of the plate is raised to T_w. The other porous plate is kept at distance H from the moving plate with the constant temperature $T_0 (T_w > T_0)$. Suction/injection with the velocity $V_0$is considered for the moving porous plate situated at $y' = 0$.

The governing momentum and energy equations in dimentional form are:

$$\rho_{nf}\left[\frac{\partial u'}{\partial t'} + V_0 \frac{\partial u'}{\partial y'}\right] = \mu_{nf} \frac{\partial^2 u'}{\partial y'^2} - \sigma B_0^2 u' + (\rho\beta)_{nf}\, g\,(T' - T_0) - \frac{\mu_{nf}}{k_0} u \qquad (1)$$

$$\left(\rho C_P\right)_{nf}\left[\frac{\partial T'}{\partial t'}+V_0\frac{\partial T'}{\partial y'}\right]=k_{nf}\frac{\partial^2 T'}{\partial y'^2}-\frac{\partial q_r}{\partial y'} \tag{2}$$

Appropriate boundary conditions are

$$t'\le 0:\ u'=0,\ \ T'=T_0,\ \ 0\le y\le H$$

$$t'\ge 0:\ \begin{cases}u'=U,\ \ T'=T_w,\ \ at\ \ y'=0\\ u'=0,\ \ T'=T_0,\ \ at\ \ y'=H\end{cases} \tag{3}$$

where, t' and u' are time and fluid velocity in the y' direction, g is the gravitational acceleration, T' is the dimensional temperature of the fliud, σ is the fluid electrical conductivity, k_0 is the permeability coefficient.

μ_{nf}, ρ_{nf}, ν_{nf}, k_{nf}, β_{nf} and $\left(\rho C_P\right)_{nf}$ are effective dynamic viscosity, effective density, effective kinematic viscosity, thermal conductivity, thermal expension and the heat capacitance of the nanofluid,which are defined asfollows [27]:

$$\mu_{nf}=\frac{\mu_f}{\left(1-\phi\right)^{2.5}},\ \rho_{nf}=\left(1-\phi\right)\rho_f+\phi\rho_s,\ \nu_{nf}=\frac{\mu_{nf}}{\rho_{nf}},\ \left(\rho\beta\right)_{nf}=\left(1-\phi\right)\left(\rho\beta\right)_f+\phi\left(\rho\beta\right)_s,$$

$$\frac{k_{nf}}{k_f}=\frac{\left(k_s+\left(n-1\right)k_f\right)-\phi\left(n-1\right)\left(k_f-k_s\right)}{\left(k_s+\left(n-1\right)k_f\right)+\phi\left(k_f-k_s\right)},\ \left(\rho C_P\right)_{nf}=\left(1-\phi\right)\left(\rho C_P\right)_f+\phi\left(\rho C_P\right)_s, \tag{4}$$

where, ϕ is the solid volume fraction of nanofluid, $\rho_f,\mu_f,k_f,\beta_f,\left(\rho C_P\right)_f$ are reference density, dynamic viscosity, thermal conductivity, thermal expension and heat capacitance of base fluid, respectively. $\rho_s,\mu_s,k_s,\beta_s,\left(\rho C_P\right)_s$ are reference density, dynamic viscosity, thermal conductivity, electrical conductivity and heat capacitanceof solid fractions, respectively. To measure the thermal conductivity of the nanofluid, k_{nf} for different shapes of nano particles, we adopted the following formula which is given by Hamilton and Crosser[30]. Here n is the nano particle shape, for spherical *n*=3 and for cyildrical shapd particles n=3/2. Here we take spherical shaped nano particles. The subscript nf denotes nanofluid, f reprsents the base fluid and s denote solid nanoparticle.

For radiation effect, we use Rosseland diffusion approximiation

$$q_r = -\frac{4\sigma_1}{3k_1}\frac{\partial T'^4}{\partial y'}$$

where σ_1 is the Stefan–Boltzmann constant and k_1 is the mean absorption coefficient. We assumed that the temperature differences within the flow are such that the term T^4 may be expressed as a linear function of temperature. This is accomplished by expanding T^4 in a Taylor series about T_0 and neglecting second and higher order terms, we get

$$T^4 \cong 4T_0^3 T' - 3T_0^4$$

$$\frac{\partial q_r}{\partial y'} = \frac{\partial}{\partial y'}\left(\frac{-4\sigma_1}{3k_1}\frac{\partial T'^4}{\partial y'}\right) = \frac{\partial}{\partial y'}\left(\frac{-4\sigma_1}{3k_1}\frac{\partial\left(4T_0^3T' - 3T_0^4\right)}{\partial y'}\right) = \frac{-16\sigma_1 T_0^3}{3k_1}\frac{\partial^2 T'}{\partial y'^2} \qquad (5)$$

The physical properties of the Cu particles and base fluid(Ethylene Glycol) are shown in Table 1.

Introducing the dimensionless quantities for converting the present problem in dimentionaless form are

$$t = \frac{t'\nu_{nf}}{H^2}, \quad y = \frac{y'}{H}, \quad u = \frac{u'}{U}, \quad \theta = \frac{T' - T_0}{T_w - T_0},$$

where, *t*, *u* and θ are nondimentional time, velocity and temperature. The magnetic parameter, Prandtl number, suction/injection parameter, Grashoff number, radiation parameter and porosity parameter are defined respectively, as follows:

$$M^2 = \frac{\sigma B_0^2 H^2}{\rho_f \nu_f}, \quad \Pr = \frac{k_f}{\left(\nu\rho C_P\right)_f}, \quad S = \frac{V_0 H}{\nu_f}, \quad Gr = \frac{g\beta_f H^2\left(T_w - T_0\right)}{U\nu_f},$$

$$N = \frac{4\sigma_1 T_0^3}{k_1 k_f}, \quad K = \frac{k_0}{H^2} \qquad (6)$$

By using equations (4-6) in equations (1-3), we get the non-dimentional form of momentum and energy equations with respective boundary conditions as follows:

$$\phi_1\phi_2\left[\frac{\partial u}{\partial t} + S\frac{\partial u}{\partial y}\right] = \frac{\partial^2 u}{\partial y^2} + Gr\phi_1\phi_3\theta - \phi_1 M^2 u - \frac{u}{K} \qquad (7)$$

$$\Pr \phi_4 \left[\frac{\partial \theta}{\partial t} + S \frac{\partial \theta}{\partial y} \right] = \left(\frac{k_{nf}}{k_f} + \frac{4N}{3} \right) \frac{\partial^2 \theta}{\partial y^2} \tag{8}$$

with the dimensionless initial and boundary conditions as

$$t \le 0: \; u = 0, \;\; \theta = 0, \;\; 0 \le y \le 1$$

$$t \ge 0: \; \begin{cases} u = 1, \;\; \theta = 1, \;\; at \;\; y = 0 \\ u = 0, \;\; \theta = 0, \;\; at \;\; y = 1 \end{cases} \tag{9}$$

where

$$\phi_1 = (1-\phi)^{2.5}, \; \phi_2 = 1-\phi+\phi\left(\frac{\rho_s}{\rho_f} \right), \; \phi_3 = 1-\phi+\phi\frac{(\rho\beta)_s}{(\rho\beta)_f}, \; \phi_4 = 1-\phi+\phi\frac{(\rho C_P)_s}{(\rho C_P)_f}.$$

Method of Solution

In order to solve these unsteady, non linear momentum and energy equations (7) and (8) subject to the initial and boundaryconditions (9) Crank-Nicolson implicit finite difference scheme [31] are employed. In recent years partial differential equations has been solved by this method and thismethod is considered as one of the most reliable procedures. It is unconditionallystable. It utilizes a central differencing procedure for space and is an implicit method. Thepartial differential terms are converted to difference equations and the resulting algebraicproblem is solved using a tridiagonal matrix algorithm. For transient problems a trapezoidalrule is utilized and provides second-order convergence. The Crank–Nicolson Method (CNM)scheme has been used in numerous heat transfer, radiation and convection flow problems. The computational domain $(0 < t < \infty)$ and $(0 < y < 1)$ is divided into a mesh of lines parallel to tand yaxes.

The finite difference equations corresponding to Eqs. (7)–(8) are as follows:

$$\phi_1\phi_2 \left[\frac{u_{i,j+1} - u_{i,j}}{\Delta t} \right] + S\phi_1\phi_2 \left[\frac{u_{i+1,j+1} - u_{i,j+1} + u_{i+1,j} - u_{i,j}}{2\Delta y} \right] =$$

$$\left[\frac{u_{i-1,j+1} - 2u_{i,j+1} + u_{i+1,j+1} + u_{i-1,j} - 2u_{i,j} + u_{i+1,j}}{2(\Delta y)^2} \right] + Gr\phi_1\phi_3 \left[\frac{\theta_{i,j+1} + \theta_{i,j}}{2} \right] - \left(\phi_1 M^2 + \frac{1}{K} \right) \left[\frac{u_{i,j+1} + u_{i,j}}{2} \right]$$

(10)

$$\Pr \phi_4 \left[\frac{\theta_{i,j+1} - \theta_{i,j}}{\Delta t} \right] + \Pr S \phi_4 \left[\frac{\theta_{i+1,j+1} - \theta_{i,j+1} + \theta_{i+1,j} - \theta_{i,j}}{2\Delta y} \right] = \left(\frac{k_{nf}}{k_f} + \frac{4N}{3} \right) \left[\frac{\theta_{i-1,j+1} - 2\theta_{i,j+1} + \theta_{i+1,j+1} + \theta_{i-1,j} - 2\theta_{i,j} + \theta_{i+1,j}}{2(\Delta y)^2} \right] \tag{11}$$

Here, the subscript *i* classify the grid point along the y-direction, *j* along the t-direction. An appropriate mesh size consideredfor the calculation step sizes $\Delta t = 0.001$ and $\Delta y = 0.01$ for t and y, respectively. The values of u and θ are known at all grid points at t = 0 from the initialconditions. With the help of the known valuesat pervious time level (j), the computations of u and θ at time level (j+1) are calculated.

The finite difference equations (10)-(11) are transformed to the following algebraic equations:

$$u_{i+1,j+1}\left[\phi_1\phi_2 S\lambda\Delta y - \lambda\right] + u_{i,j+1}\left[2\phi_1\phi_2 - \phi_1\phi_2 S\lambda\Delta y + 2\lambda + \Delta t\phi_1 M^2 + \frac{\Delta t}{K}\right] - \lambda u_{i-1,j+1} = u_{i+1,j}\left[\lambda - \phi_1\phi_2 S\lambda\Delta y\right] + u_{i,j}\left[2\phi_1\phi_2 + \phi_1\phi_2 S\lambda\Delta y - 2\lambda - \Delta t\phi_1 M^2 - \frac{\Delta t}{K}\right] + \lambda u_{i-1,j} + S_{i,j} \tag{12}$$

$$\theta_{i+1,j+1}\left[\Pr\phi_4 S\lambda\Delta y - \left(\frac{k_{nf}}{k_f} + \frac{4N}{3}\right)\lambda\right] + \theta_{i,j+1}\left[2\Pr\phi_4 - \Pr\phi_4 S\lambda\Delta y + 2\left(\frac{k_{nf}}{k_f} + \frac{4N}{3}\right)\lambda\right] - \left(\frac{k_{nf}}{k_f} + \frac{4N}{3}\right)\lambda\theta_{i-1,j+1} = \theta_{i+1,j}\left[\left(\frac{k_{nf}}{k_f} + \frac{4N}{3}\right)\lambda - \Pr\phi_4 S\lambda\Delta y\right] + \theta_{i,j}\left[2\Pr\phi_4 + \Pr\phi_4 S\lambda\Delta y - 2\left(\frac{k_{nf}}{k_f} + \frac{4N}{3}\right)\lambda\right] + \left(\frac{k_{nf}}{k_f} + \frac{4N}{3}\right)\lambda\theta_{i-1,j} \tag{13}$$

where, $\lambda = \dfrac{\Delta t}{(\Delta y)^2}$ and $S_{i,j} = \Delta t Gr \phi_1 \phi_2 \left(\theta_{i,j+1} + \theta_{i,j}\right)$

under the initial and boundary conditions

$$\left.\begin{aligned} u_{i,j} &= 0, \quad i = 1,2,.....,q+1, \\ u_{1,j} &= 1 \\ u_{q+1,j} &= 0 \end{aligned}\right\} \quad j = 2,3,....., p+1, \tag{14}$$

$$\left.\begin{aligned}\theta_{i,j} &= 0, \qquad i = 1,2,.....,q+1,\\ \theta_{1,j} &= 1\\ \theta_{q+1,j} &= 0\end{aligned}\right\} \quad j = 2,3,....., p+1. \tag{15}$$

With the reference of [16],the finite difference equation (8) at every internal nodal point on a particular i - level constitutea tri-diagonal system of equations. Such a system of equations is solved by Thomas algorithmas described in [16]. Thus, the values of θ are found at every nodal point on a particular i at$(j+1)th$time level . Similarly, the values of uare calculated from the equation of (8). Thus the values of u and θ are known on a particular$i$-level. This process is repeated for various i - levels. Thus,the values of u and θ are known at all grid points in the rectangular region at $(j+1)th$time level. Computations are carried out untilthe steady state is reached. The steady state solutionis assumed to have been reached, when the absolutedifference between the values of velocity u as well as temperature θ at two consecutivetime steeps are less than 10^{-5} at all grid points.

Perticular Case: Steady state

We have converted present problem in steady state and solved analytically.

The steady state equations with boundary conditions are:

$$\frac{d^2u}{dy^2} - S\phi_1\phi_2\frac{du}{dy} - \left(\phi_1 M^2 + \frac{1}{K}\right)u = -Gr\phi_1\phi_3\theta \tag{16}$$

$$\left(\frac{k_{nf}}{k_f} + \frac{4N}{3}\right)\frac{d^2\theta}{dy^2} - \phi_4 S\,\mathrm{Pr}\frac{d\theta}{dy} = 0 \tag{17}$$

The boundary conditions are

$$u = 1, \quad \theta = 1 \quad at \quad y = 0$$

$$u = 0, \quad \theta = 0 \quad at \quad y = 1 \tag{18}$$

Anaytical Solution

The solution of equations (16-17) under the boundary conditions (18) for non-dimentional velocity and temperature profile as follows:

$$\theta = C_1 e^{sy} + C_2 \tag{19}$$

$$u = e^{a_4 y}\left[C_3 \cosh\left(a_5 y\right) + C_4 \sinh\left(a_5 y\right)\right] + a_8 e^{sy} + a_9 \tag{20}$$

Where,

$$C_1 = \frac{1}{1-e^s}, \quad C_2 = \frac{-e^s}{1-e^s}, \quad C_3 = 1 - a_8 - a_9, \quad C_4 = \frac{a_{11}}{\sinh\left(a_5\right)}$$

$$a = \frac{k_{nf}}{k_f} + \frac{4N}{3}, \quad b = \phi_4 S\,\mathrm{Pr}, \quad s = \frac{b}{a}, \quad a_1 = S\phi_1\phi_2, \quad a_2 = \phi_1 M^2 + \frac{1}{K}, \quad a_3 = Gr\phi_1\phi_3,$$

$$a_4 = \frac{a_1}{2}, \quad a_5 = \frac{\sqrt{a_1^2 + 4a_2}}{2}, \quad a_6 = -a_3 C_1, \quad a_7 = s^2 - a_1 s - a_2, \quad a_8 = \frac{a_6}{a_7},$$

$$a_9 = \frac{a_3 C_2}{a_2}, \quad a_{10} = -a_8 e^s - a_9, \quad a_{11} = \frac{a_{10}}{e^{a_4}} - C_3 \cosh\left(a_5\right)$$

Results and discussion

The influence of various parameters such as magnetic field parameter (M), permeability parameter (K), radiation parameter (N), volume fraction of nanoparticles (ϕ), Grashof number (Gr), suction parameter (S) on velocity and temperature distribution in both cases, i.e. for steady and unsteady problem are presented in the Figs. (2-10). The Prandtl number of base fluid (water) is kept on 6.2. The constant $S = 0.5(>0)$ represents injection at the plate $y' = 0$ and simultaneous suction at $y' = H$, while $S = -0.5(<0)$ corresponds to suction at the plate $y' = 0$ and simultaneous injection at $y' = H$. When $\phi = 0$ the model contracts to the governing equations for a regular viscous fluid i.e. nanoscale characteristics are eliminated.

Figs. (2-3) represent the effect of radiation parameter (N) and volume fraction (ϕ) respectively on temperature of nanofluidflow for both the situations i.e. suction/injecton at moving plate. It is observed that temperature increases as N or ϕ increases, for both suction/injection in unsteady state as well as for suction in steady state, because increase in the radiation parameter provides more heat to fluid that cause an enhancement in the temperature and thermal boundary layer thickness, but it should be notice that when injection is applied on moving plate (S>0) in steady state temperature decreases as N or ϕ increases.

The influence of dimensionless time t on temperature profile and velocity profiles are illustrated in Figs. (4-5) for injection as well for suction at $y = 0$. It is noticed that the field velocity and temperature both increases with the increament in time until it attains its steady state. Furthermore, temperature variation in Fig. 4 shows prominent effect of t,in case of injection at $y = 0$ as compared with suction at $y = 0$.

From Fig. 6(a-b) it is noted that variation in permeability of the porous medium K shows prominent effect on steady state velocity when either injection or suction is applied at $y = 0$. Further velocity increases as permeability parameter increases, butthis increamnet insignificiant at higher permeability.It is due to the reason that Darcy's resistance force decreases as permeability increases, therefore flow increases.

Transient and steady state velocity of nanofluid decreases as magnetic field parameter M increases, which can be seen from Fig. 7 (a-b) in both case, i.e. when $S>0$ and $S<0$. This is because the presence of magnetic field in an electrically conducting fluid introduces a force called the Lorentz force, which acts against the flow if the magnetic field is applied perpendicular to the flow direction.

The effect of volume fraction paramter ϕ on velocity distribution for both steady and unsteady state is presented in Fig. 8 (a-b). The result shows that flow velocity reduces when volume fraction of nanoparticles is increased in both states, but the role of ϕ is insignificant on velocity in case of unsteady state for both situation when injection is applied at moving plate and suction is on stationary plate or vice-versa.

Fig. 9 (a-b) depicts the effect of Grashof number Gr on velocity distribution under the influence of injection and suction respectively. For both the states increasing value of Gr enhance the steady and unsteady velocity. Also the effect of Gr is more significant in steady state as comparedwith transient state in both Figs. 9(a) and 9(b). From Fig. 10 (a-b) we can see that both the steady and unsteady state velocity diminishas radiation parameter increases when $S>0$ (injection) at $y = 0$ and it shows reverse effect for $S<0$ (suction) at $y = 0$.

Conclusion

We have investigated free convective MHD Couette flow of nanofluid between a vertical permeable channel in the prsence of thermal radiation effect and suction/injection through porous medium. The investigation is done for both steady and unsteady flow and heat tranfer under same boundary conditions. We have observed that:

- For both situations suction/injection, the field velocity and temperature both increases with the increament in time until it attains its steady state.
- For both suction/injection, velocity profile increases with increasing effect of permeability paramter K and Grashof number Gr, while reverse effect shows in increament of magnetic paramter M and volume fraction paramter ϕ.
- When we applied suction, temperature enhanced with increasing effect of radiation and volume fraction for both steady and unsteady states, but in case of injection temperature increases in unsteady whereas in steady state it reduces .

Conflict of Interests

The authors declare that there is no conflict of interests regarding the publication of this paper.

References

1) Kumar J P, Umavathi J C,Chamkha A J& PopI, *ApplMathModel*, 34 (2010)1175.
2) Umavathi J C,Kumar J P, Chamkha A J & Pop I, *Transport Porous Med*, 61(2005)315.
3) Hussanan A, Salleh M,Tahar R&Khan I, *PLoS ONE* 9(10) (2014) e108763.
4) Khalid A, Khan I, Khan A&Shafie S,*Eng Sci Technol IntJ*, 18 (2015)309.
5) Khem C, Rakesh K &Shavnam S, *Int J PhysMath Sci*, 3 (1) (2012) 82.
6) Jha B K, Singh A K, & Takhar H S, *Int ApplMechEng*, 8(3) (2003) 497.
7) Jha B K,Samaila A K &Ajibade A O, *Comput Math Model* 24(3)(2013) 432.
8) Kataria H R &Patel H R, *Alexandria Eng J*, 55 (2016) 583.
9) Kataria H R &Patel H R, *Alexandria Eng J*, (2016) xxx, xxx–xxx.
10) Attia A H, *Kragujevac J Sci*,32 (2010), 17.
11) RundoraL &Makinde O D, *J Petrol Sci Eng*, 108 (2013) 328.
12) Jha B K, Isah B Y &Uwanta I J, *J King Saud Univ Sci*, 27 (2015) 338.
13) Jha B K, Isah B Y &Uwanta I J, *AinShams Engg J*,2016 xxx, xxx–xxx.
14) Maxwell J C, *2nd edn. Clarendon Press, Oxford* 1981.
15) Choi S U S & Eastman J A, *Materials Sci*, 231 (1995) 99.
16) BuddakkagariV &Kumar M, *Int J Appl Comput Math*, 1 (2015) 427.
17) Chauhan D S &Kumar V, *Appl Math Sci*, 6(36) (2012) 1759.
18) Baoku I G, Israel-Cookey C & Olajuwon B I, *Surv MathAppl*, 5 (2012) 215.

19) Chauhan D S &Rastogi P, *J Appl SciEng*, 15 (3) (2012) 281.
20) Chauhan D S &Kumar V, *Therm Sci*, 15 (2003) S175.
21) Jain S, Kumar V& Bohra S, *Int J Energy & Tech*, 7 (2015) 40.
22) Hazem A A,*Kragujevac J Sci*, 32, 17–24, 2010b.
23) Ibrahim W &Shankar B, *JFluids Eng*, 134(8) (2012) 081203.
24) Kumari M, Gorla R S R, *J Nanofluids*, 1(2) (2012) 166.
25) Raju C S K,Babu M J, Sandeep N, SugunammaV &Reddy J V R, *Chem ProcessEngg Research*, 30 (2015) 9.
26) Mohankrishna P, SugunammaV &SandeepN, *Chem Process Engg Research*, 25 (2014) 39.
27) Rajesh V, Mallesh M P &Bég O A, *Procedia Materials Sci*, 10 (2015) 80.
28) Gorla R S R &Chamkha A J, *ThermophyEngg*, 15(2) (2011) 81.
29) Jain S & Bohra S, *Adv Math Phys*,(2016)1.
30) Elsaid EM, Abdel-wahed MS, *Therm Eng*, 25 (2021) 100913.
31) Atashafrooz M, *J Therm Anal Calorim*, 138 (2019) 3109.
32) Alizadeh R, Karimi N, Arjmandzadeh R & Mehdizadeh A, *J Therm Anal Calorim*, 135 (2019) 489.
33) Qasim M& Ashraf MU, *Alexandria Eng J*, 60(3) (2021) 3305.
34) Hamilton R L &Crosser O K, *J Ind Eng Chem Fundum*, 1(3) (1962) 187.
35) Crank J & Nicolson P, *Proc CambPhil Soc*, 43 (1947) 50.

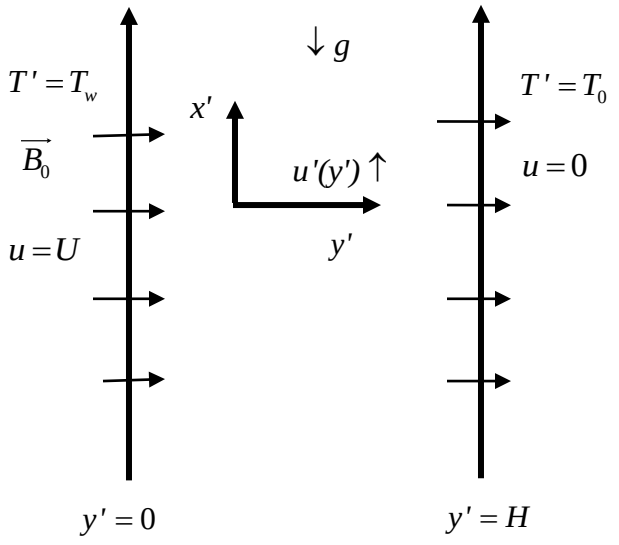

Fig. 1. Physical configuration and coordinate system.

a) b)

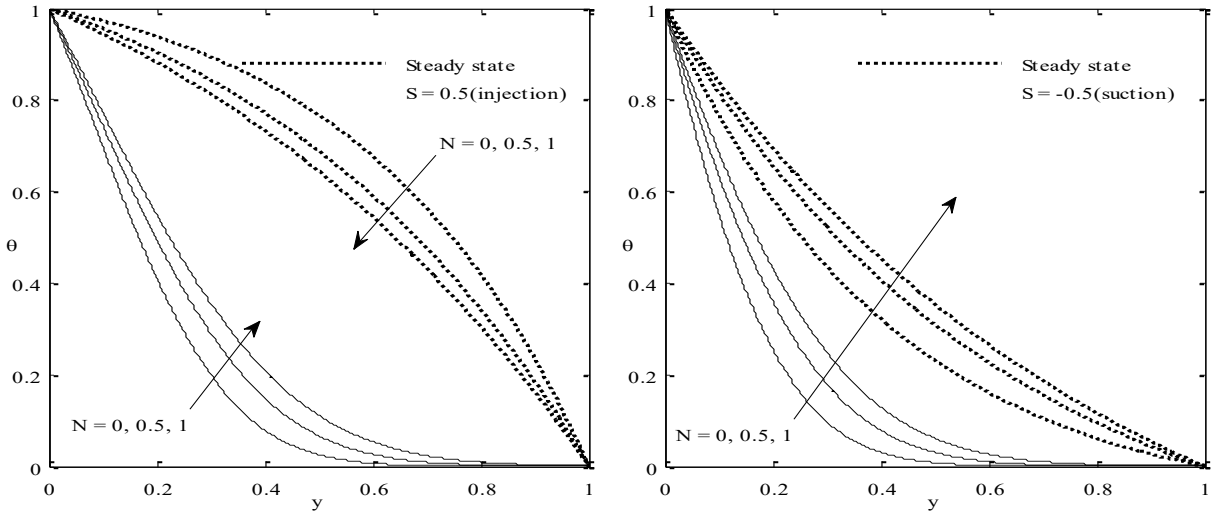

Fig. 2 Effect of variation inradiation parameter N in (**a**) Injection (*S*> 0) (**b**) Suction (*S*< 0) on the temperature profile when Pr = 6.2, time t = 0.1, ϕ = 0.1

a) b)

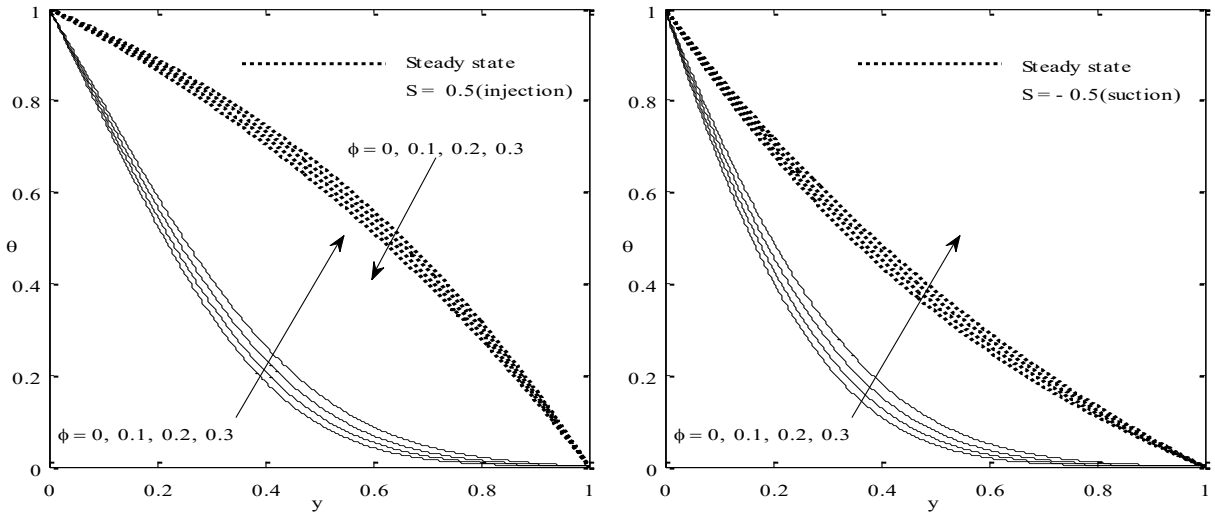

Fig. 3 Effect of variation inradiation parameter N (**a**) Injection (*S*> 0) (**b**) Suction (*S*< 0) on the temperature profile when Pr = 6.2, time t = 0.1, N=1

a) b)

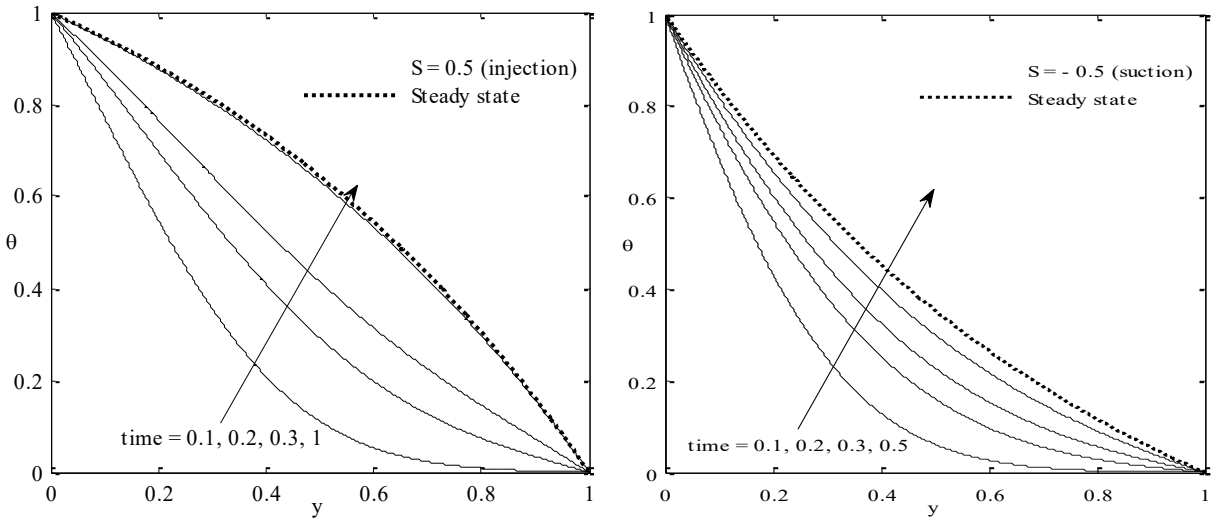

Fig. 4 Effect of variation intime t (**a**) Injection (*S*> 0) (**b**) Suction (*S*< 0) on the temperature profile when Pr = 6.2, N =1, ϕ = 0.1

a) b)

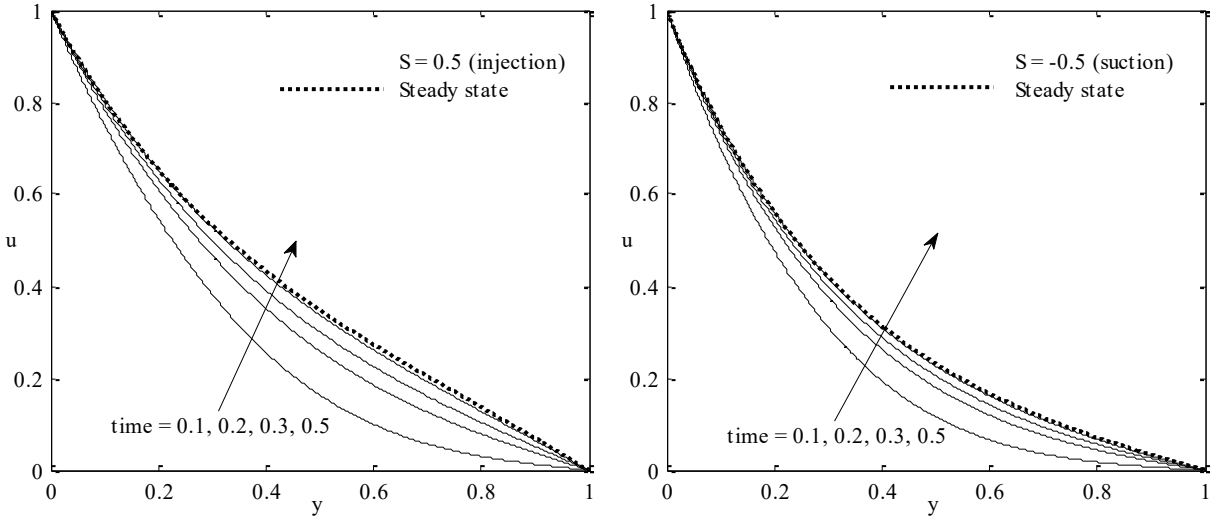

Fig. 5 Effect of variation intime t (**a**) Injection (*S*> 0) (**b**) Suction (*S*< 0) on the velocity profile when Pr = 6.2, ϕ = 0.1, M = 1, K = 0.1, Gr = 5, N = 1

a) b)

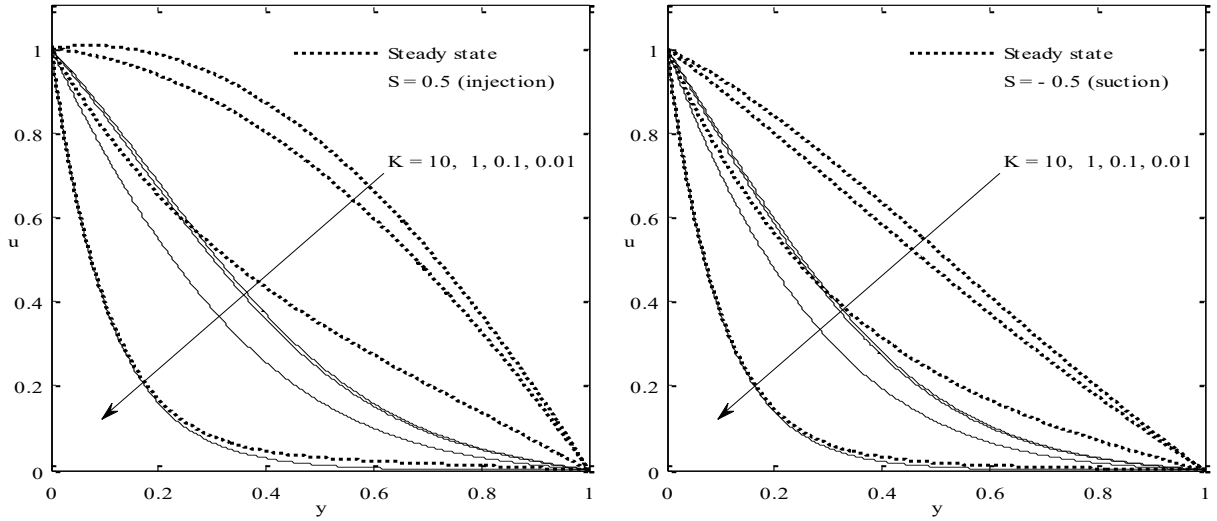

Fig. 6 Effect of variation inpermeability parameter K (**a**) Injection (*S*> 0) (**b**) Suction (*S*< 0) on the velocity profile when Pr = 6.2, ϕ = 0.1, M = 1, t = 0.1, Gr = 5, N = 1

a) b)

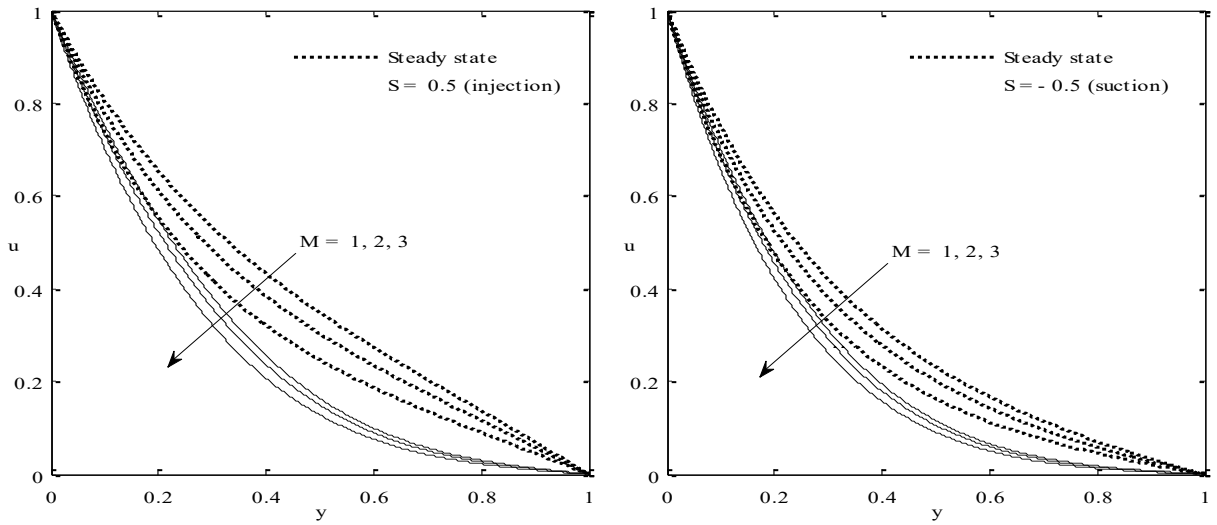

Fig. 7 Effect of variation inmagnetic parameter M (**a**) Injection (*S*> 0) (**b**) Suction (*S*< 0) on the velocity profile when Pr = 6.2, ϕ = 0.1, K = 0.1, t = 0.1, Gr = 5, N = 1

a) b)

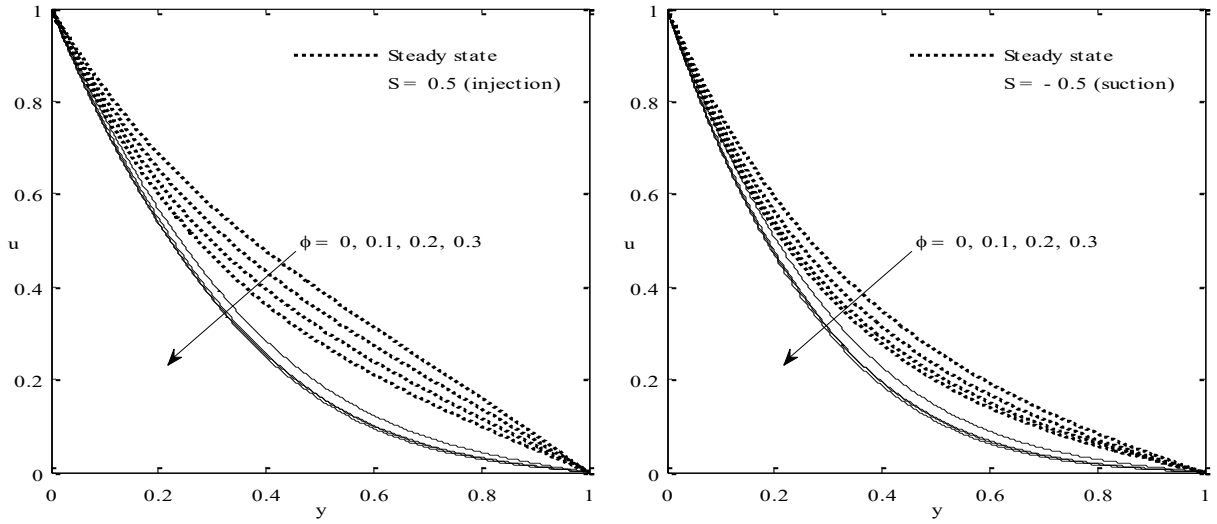

Fig. 8 Effect of variation involume fraction of nanofluid ϕ(**a**) Injection (*S*> 0) (**b**) Suction (*S*<0) on the velocity profile when Pr = 6.2, M = 1, K = 0.1, t = 0.1, Gr = 5, N = 1

a) b)

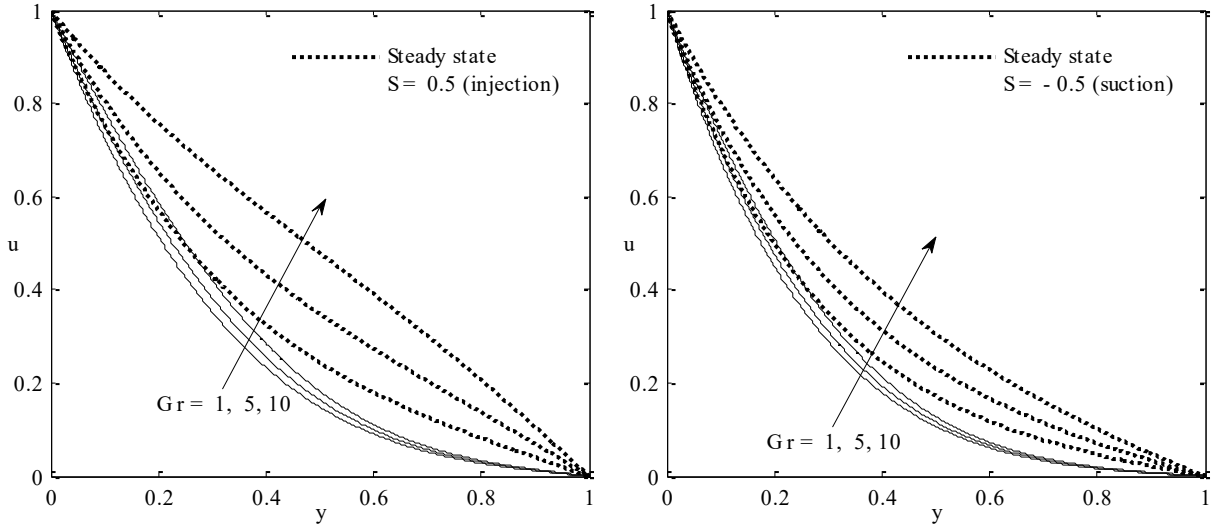

Fig. 9 Effect of variation inGrashoff number Gr (**a**) Injection (*S*> 0) (**b**) Suction (*S*< 0) on the velocity profile when Pr = 6.2, ϕ = 0.1, K = 0.1, t = 0.1, M = 1, N = 1

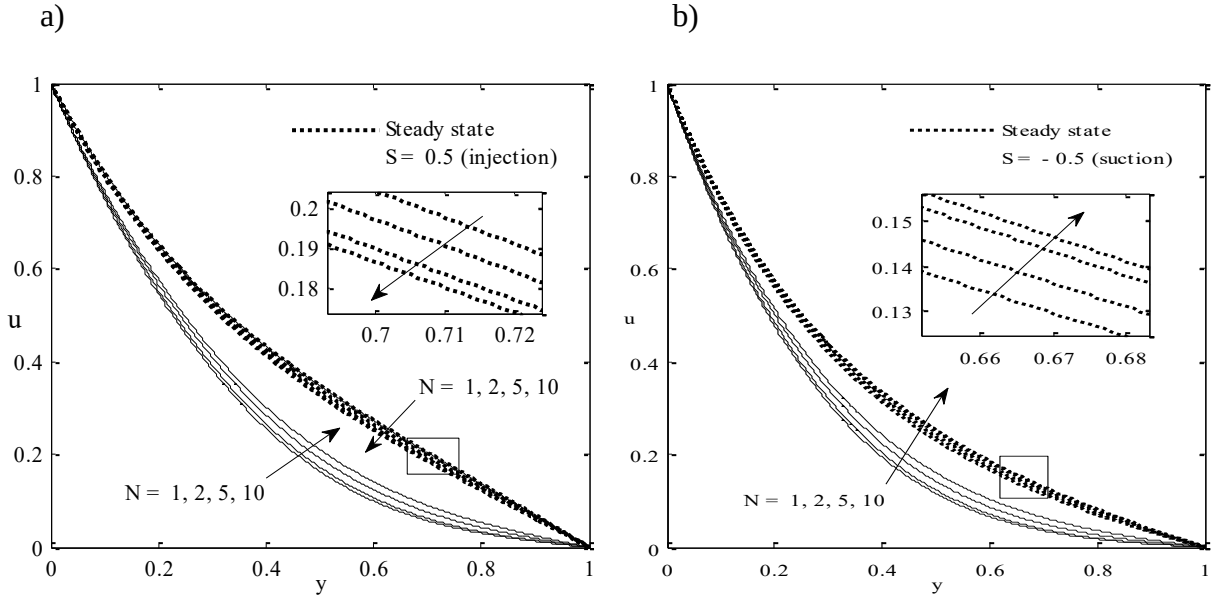

Fig. 10 Effect of variation in radiation parameter N (**a**) Injection (*S*> 0) (**b**) Suction (*S*< 0) on the velocity profile when Pr = 6.2, ϕ = 0.1, K = 0.1, t = 0.1, M = 1, Gr = 5

Table 1 Thermophysical properties of fluid and nanoparticles [25]

Physical properties	Ethylene Glycol	Cu (Copper)
***Cp* (J/kg K)**	2415	385
ρ (kg/m3)	1114	8933
***k*(W/m K)**	0.252	400
β (1/ K)	57×10^{-5}	1.67×10^{-5}